

Thermodynamic Space of Chemical Reaction Networks

Shiling Liang (梁师翎)^{1,*} Paolo De Los Rios^{1,2} and Daniel Maria Busiello^{3,†}

¹*Institute of Physics, School of Basic Sciences, École Polytechnique Fédérale de Lausanne (EPFL), 1015 Lausanne, Switzerland*

²*Institute of Bioengineering, School of Life Sciences,*

École Polytechnique Fédérale de Lausanne (EPFL), 1015 Lausanne, Switzerland

³*Max Planck Institute for the Physics of Complex Systems, 01187 Dresden, Germany*

(Dated: July 17, 2024)

Living systems are usually maintained out of equilibrium and exhibit complex dynamical behaviors. The external energy supply often comes from chemical fluxes that can keep some species concentrations constant. Furthermore, the properties of the underlying chemical reaction networks (CRNs) are also instrumental in establishing robust biological functioning. Hence, capturing the emergent complexity of living systems and the role of their non-equilibrium nature is fundamental to uncover constraints and properties of the CRNs underpinning their functions. In particular, while kinetics plays a key role in shaping detailed dynamical phenomena, the range of operations of any CRN must be fundamentally constrained by thermodynamics, as they necessarily operate with a given energy budget. Here, we derive universal thermodynamic upper and lower bounds for the accessible space of species concentrations in a generic CRN. The resulting region determines the “thermodynamic space” of the CRN, a concept we introduce in this work. Moreover, we obtain similar bounds also for the affinities, shedding light on how global thermodynamic properties can limit local non-equilibrium quantities. We illustrate our results in two paradigmatic examples, the Schlögl model for bistability and a minimal self-assembly process, demonstrating how the onset of complex behaviors is intimately tangled with the presence of non-equilibrium driving. In summary, our work unveils the exact form of the accessible space in which a CRN must work as a function of its energy budget, shedding light on the non-equilibrium origin of a variety of phenomena, from amplification to pattern formation. Ultimately, by providing a general tool for analyzing CRNs, the presented framework constitutes a stepping stone to deepen our ability to predict complex out-of-equilibrium behaviors and design artificial chemical reaction systems.

I. INTRODUCTION

Living systems operate far from equilibrium, consuming energy to maintain organized states against the tendency toward increasing entropy [1]. This intrinsic non-equilibrium nature of life is sustained by biological processes fundamentally built on chemical reactions [2]. Chemical reaction networks (CRNs) capture many of these biochemical processes, including gene regulation, metabolism, and cellular information processing [3–6]. To analyze these complex systems, chemical reaction network theory has been developed, providing a powerful framework for characterizing CRNs and revealing how complex behaviours emerge from underlying molecular interactions [4, 7]. This complexity manifests in various forms, including non-equilibrium stationary state, multistationarity, chaos, and oscillations [8–12]. This wide spectrum of possibilities is instrumental for establishing robust biological functions, together with the necessity of continuously harvesting and dissipating energy into the environment. Indeed, non-equilibrium conditions play a leading role in determining the operations of a biological

system, e.g., they can amplify the abundance of a desired biochemical state [13–17], trigger the onset of complex dynamics [10, 18], and regulate the emergence of large-scale structures [19–21].

Due to its relevant role, a thermodynamically consistent chemical reaction theory has been developed to describe the thermodynamics of these systems in and out of equilibrium by quantifying the irreversibility of fluxes and relating it to free energy change [22–26]. Recent works focused on the role of the topology of CRNs in shaping their non-equilibrium behaviors, studying, for example, the properties of dissipative fluxes due to external chemostats, i.e., devices that fix the concentrations of selected chemical species [27, 28], deriving thermodynamic bounds on perturbation responses [29], and characterizing how chemical systems tune efficiency [30].

Despite the undoubted relevance of understanding out-of-equilibrium phenomena, the general constraints that thermodynamic drivings of any source can impose on biochemical systems are still elusive. In particular, revealing how global non-equilibrium properties constrain specific physical observables and shape the range of operations of CRNs is a formidably hard challenge. Recent studies have provided valuable insights into linear and catalytic chemical networks [20, 31], shedding light on the thermodynamic constraints on non-equilibrium amplifi-

* shiling.liang@epfl.ch

† busiello@pks.mpg.de

cation, accuracy of information processing, and contrast in reaction-diffusion patterns [20, 32, 33]. However, these analyses have been limited to (pseudo-)unimolecular CRNs that can always be represented by simple graphs whose steady state can be represented in terms of pseudo-equilibrium solutions to reveal their thermodynamic features (employing the matrix-tree theorem [34, 35]). It remains the question of how these principles apply to more generic CRNs involving multi-molecular reactions where the topology of the networks is represented by hypergraphs [28, 36].

In this work, we tackle this problem and extend these ideas to generic CRNs, deriving fundamental thermodynamic bounds on reaction affinities and species concentrations. Our approach goes beyond previous studies by solving the challenging task of considering CRNs with arbitrary network topologies. This is indeed a crucial step allowing for the application of our results to fields in which complex multimolecular reactions are usually involved, such as metabolic networks and self-assembly systems. To this end, we introduced the key concept of *thermodynamic space*, which is the accessible phase space of concentrations within which a biochemical system must operate at stationarity. By providing a general framework for understanding the thermodynamic limits of CRNs, our work opens new avenues for predicting and analyzing complex behaviors in a wide range of biological and synthetic chemical systems. As pedagogical yet non-trivial examples, we illustrate the applicability of our findings to the bi-stable Schogl model and a simple self-assembly scheme involving the creation of chemical complexes.

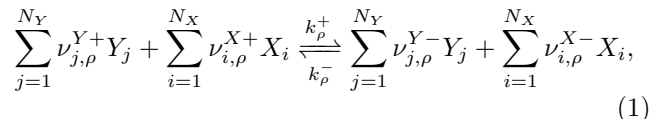
The paper is structured as follows: In Sec. II, we introduce the basic concepts of the thermodynamically-consistent modeling of generic CRNs, including basic definitions to characterize network topology and conservation laws. In Sec. III, we present our main results: thermodynamic constraints on reaction affinities and species concentrations at stationarity. To assess thermodynamic constraints on arbitrary sets of chemical species, we introduce the concept of “chemical probe” - an artificial reaction that plays a role analogous to a voltmeter in an electric circuit. This probe allows us to evaluate the thermodynamic accessible space for concentrations of species involved in any possible reaction compatible with the conservation laws. In Sec. IV, we apply our thermodynamic bounds to several representative CRNs to demonstrate their implications and broad applicability.

II. THERMODYNAMICS AND GEOMETRY OF CHEMICAL REACTION NETWORKS

A. Dynamics and Local Detailed Balance (LDB)

A CRN describes a set of interconnected reactions converting chemical species. In this study, we focus on open CRNs maintained out-of-equilibrium through

chemostats. These are devices that provide a continuous influx and outflux of specific chemical species, keeping their concentrations fixed in time. Within this framework, we categorize the chemical species $\{Z_\sigma\}$ into two distinct types: internal species $\{X_i\}_{i=1,\dots,N_X}$, whose concentrations are governed by the reaction dynamics within the network, and external (chemostatted) species $\{Y_j\}_{j=1,\dots,N_Y}$, which are maintained at constant concentrations by the action of chemostats. Let ρ denote the index of one of the N_R possible reactions in the CRN. We can represent a generic reaction in the following form:



where $\nu_{i,\rho}^{X+}$, $\nu_{i,\rho}^{X-}$ denote the stoichiometric coefficients of the internal species X_i in the forward and reverse reactions, respectively. Here, $\nu_{j,\rho}^{Y+}$, $\nu_{j,\rho}^{Y-}$ represent the same quantities for the external species Y_j . The rate constants for the forward and reverse reaction are respectively given by k_ρ^+ and k_ρ^- . As discussed later, to ensure thermodynamic consistency, we consider all chemical reactions to be bidirectional, i.e., reversible CRNs. The stoichiometric changes induced by all reactions in the network are captured by the stoichiometric matrix \mathbb{S} :

$$\mathbb{S} = \begin{pmatrix} \text{internal species} \\ \text{external species} \end{pmatrix} = \begin{pmatrix} \mathbb{S}^X \\ \mathbb{S}^Y \end{pmatrix} \quad (2)$$

where \mathbb{S}^X and \mathbb{S}^Y are two block matrices whose entries are defined by $\mathbb{S}_{i,\rho}^X = \nu_{i,\rho}^{X-} - \nu_{i,\rho}^{X+}$ and $\mathbb{S}_{j,\rho}^Y = \nu_{j,\rho}^{Y-} - \nu_{j,\rho}^{Y+}$, representing the net change in molecular numbers for internal and external species, respectively, due to the ρ -th reaction. \mathbb{S}^X has dimensions $N_X \times N_R$, while \mathbb{S}^Y is a $N_Y \times N_R$ matrix. For the sake of generality, Z_σ denotes a generic chemical species (internal or external) and $\mathbb{S}_{\sigma,\rho}$ the entry of \mathbb{S} corresponding to the change of its molecular number due to the ρ -th reaction. The ρ -th column of \mathbb{S} , denoted as \mathbb{S}_ρ , represents the change in molecular numbers for all species in the ρ -th reaction.

For dilute CRNs, the concentration evolution can be expressed through the mass-action law. In particular, we can introduce the forward and backward flux vectors, \mathbf{J}^+ and \mathbf{J}^- , whose ρ -th component quantifies the propensity of a given reaction ρ in the forward or backward direction, respectively. The explicit form follows the mass-action kinetics:

$$J_\rho^+ = k_\rho^+ \prod_{i=1}^{N_X} [X_i]^{\nu_{i,\rho}^{X+}} \prod_{j=1}^{N_Y} [Y_j]^{\nu_{j,\rho}^{Y+}} \quad (3)$$

and analogously for J_ρ^- , where $[X_\sigma]$ indicates the concentration of the species X_σ . By further introducing the net flux vector \mathbf{J} , whose element $J_\rho = J_\rho^+ - J_\rho^-$, we can express the dynamics of species concentrations in the network through the stoichiometric matrix as:

$$\frac{d\mathbf{x}}{dt} = \mathbb{S}^X \mathbf{J}, \quad \frac{d\mathbf{y}}{dt} = \mathbb{S}^Y \mathbf{J} + \mathbf{I}^Y = \mathbf{0}. \quad (4)$$

Here, we used the short-hand notation \mathbf{x} to indicate the vector of concentrations of internal species, so that its element $x_\sigma = [X_\sigma]$, and analogously for \mathbf{y} . We denote the complete set of species concentrations as $\mathbf{z} = (\mathbf{x}, \mathbf{y})$. The external flux \mathbf{I}^Y is induced by chemostats and maintains constant concentrations of chemostatted species by compensating the flux to internal chemical reactions. If the system reaches a steady state, it will satisfy the condition

$$\mathbb{S}^X \mathbf{J}^{\text{ss}} = \mathbf{0}, \quad (5)$$

where \mathbf{J}^{ss} represents the steady-state flux vector, i.e., the flux where all concentrations have been replaced by their stationary values. However, it is important to note that not all CRNs necessarily reach a steady state. Some systems may exhibit limit cycle, chaos, or other types of attractors. In this work, we restrict our discussion to the CRNs that can reach stationary state solutions.

Thermodynamics is incorporated through the local detailed balance (LDB) condition [25], which constrains the ratio of forward to backward fluxes:

$$\frac{J_\rho^+}{J_\rho^-} = e^{-\Delta_\rho G/RT} = e^{A_\rho/RT}, \quad (6)$$

where $\Delta_\rho G = \sum_\sigma \mu_{Z_\sigma} \mathbb{S}_{\sigma,\rho}$ is the free energy change along the reaction ρ , and $A_\rho = -\Delta_\rho G$ is the reaction affinity. The affinity aligns with the direction of the net reactive flux J_ρ . The chemical potential of a species Z_σ is given by $\mu_{Z_\sigma} = \mu_{Z_\sigma}^\circ + RT \ln z_\sigma$, where $\mu_{Z_\sigma}^\circ$ is the standard chemical potential and $RT \ln z_\sigma$ is the entropic contribution, again recalling that $z_\sigma = [Z_\sigma]$. We then introduce the chemical potential vector $\boldsymbol{\mu}$ whose elements $\mu_\sigma = \mu_{Z_\sigma}$. By employing this simplified notation, the affinity vector for all reactions in the network can be computed as:

$$\mathbf{A} = -\mathbb{S}^T \boldsymbol{\mu}. \quad (7)$$

where \mathbb{S}^T is the transpose of the stoichiometric matrix. By splitting the chemical potential vector into the contributions from internal and external species, $\boldsymbol{\mu} = (\boldsymbol{\mu}^X, \boldsymbol{\mu}^Y)$, the affinity can be decomposed as:

$$\mathbf{A} = \mathbf{A}^X + \mathbf{A}^Y = -(\mathbb{S}^X)^T \boldsymbol{\mu}^X - (\mathbb{S}^Y)^T \boldsymbol{\mu}^Y. \quad (8)$$

The affinity \mathbf{A}^X represents the thermodynamic driving force associated with changes in internal species, while \mathbf{A}^Y represents the thermodynamic driving force associated with changes in external species.

By taking advantage of the mass-action kinetic in Eq. (3), the LDB condition can be rewritten in terms of reaction rate constants:

$$\frac{k_\rho^+}{k_\rho^-} = e^{-\Delta_\rho G^\circ/RT}, \quad (9)$$

where $\Delta_\rho G^\circ = \sum_\sigma \mu_{Z_\sigma}^\circ \mathbb{S}_{\sigma,\rho}$ is the change in the standard free energy along the reaction ρ . This form corresponds to the LDB commonly referred to in stochastic thermodynamics [26], even if the expression in Eq. (6) can be considered to be valid more in general. We also remark that our results are solely based on Eq. (6) and not on the specific form of the kinetics.

B. Cycles and Elementary Flux Modes (EFMs)

A generic CRN can be regarded as a hypergraph in which each reaction is a hyperedge connecting multiple reaction species. The stoichiometric matrix defines the geometry of the hypergraph, from which we can extract the hypercycles as a sequence of reactions through which the system remains unchanged. From an algebraic perspective, a vector \mathbf{v} is a cycle of a CRN, i.e., it contains the set of reactions that produces no net changes in molecular numbers, if $\mathbb{S}\mathbf{v} = \mathbf{0}$, namely the vector belongs to the right nullspace of the stoichiometric matrix, also called the kernel of the matrix, $\text{Ker}(\mathbb{S})$.

For an open CRN, internal species are affected by the reaction dynamics and we are thus interested in the cycles of the stoichiometric matrix of internal reactions, \mathbb{S}^X . These cycles \mathbf{c} are vectors of size N_R , they are called “flux modes” and satisfy:

$$\mathbb{S}^X \mathbf{c} = \mathbf{0}. \quad (10)$$

This equation is solved by all possible sets of reactions that preserve the molecular numbers of internal species only. The space constituted by all flux modes is the kernel of the internal stoichiometric matrix, $\text{Ker}(\mathbb{S}^X)$. We can immediately see that, according to Eq. (5), the stationary solution \mathbf{J}^{ss} of a CRN is a flux mode. That means we can interpret the flux modes as all possible steady-state solutions for the fluxes, while the actual solution depends on the specific values of the rates.

Understanding all possible pathways through which a CRN can operate it is of fundamental importance to introduce the concept of “elementary flux modes” (EFMs). EFMs form a basis for $\text{Ker}(\mathbb{S}^X)$, so that all possible flux modes in the CRNs can be expressed as linear combinations of EFMs. Any EFM is a vector of size N_R and cannot be further decomposed into simpler cycles nor expressed through combinations of other EFMs. Algebraically, the support of an EFM, i.e., the set of indices of non-zero entries $\text{supp}(\mathbf{e}) = \{\rho \mid e_\rho \neq 0\}$, must be minimal. As such, an EFM, denoted by the vector \mathbf{e} , is a minimal flux mode that can sustain a steady-state solution. We indicate that e_ρ is the ρ -th element of the EFM \mathbf{e} and its modulus represents the number of times the reaction ρ occurs along \mathbf{e} . Moreover, the sign of e_ρ indicates whether the reaction is performed in the forward (positive) or backward (negative) direction in the EFM. Notice that this definition intrinsically depends on the arbitrary choice of the positive direction of a given reaction that we consider to be the forward one. A different choice will lead to the same result.

A key property of EFMs is that any flux mode admits a conformal decomposition, i.e., it can be written as a sum without cancellation of linearly independent EFMs [30, 37], each of them conformal to it. Consequently, since the steady-state flux \mathbf{J}^{ss} is a flux mode, it also admits a conformal decomposition. In Sec. III, we will leverage this property to prove our main results.

C. Conservation laws and reaction space

Another crucial ingredient to fully characterize a CRN is the identification of conservation laws. They are encapsulated in the left null space of \mathbb{S} , known as the cokernel of \mathbb{S} or equivalently the kernel of \mathbb{S}^T [4, 25]. We denote the set of all conservation laws as $\mathcal{L} = \text{Ker} [\mathbb{S}^T]$, which is also named “metabolic pool” in the context of metabolic networks [38]. Hence, for any conservation law $\mathbf{l} \in \mathcal{L}$ of a CRN, $\mathbf{l}^T \mathbb{S} = \mathbf{0}$ holds. In an open CRN, the introduction of chemostats breaks some conservation laws, particularly those involving chemostatted species $\{Y_j\}_{j=1, \dots, N_Y}$ [27]. Consequently, only a subspace of \mathcal{L} represents conserved quantities in an open system. This subspace, denoted by \mathcal{L}^X is exactly the cokernal of \mathbb{S}^X , i.e., $\mathcal{L}^X = \text{Ker} [(\mathbb{S}^X)^T]$. For any $\mathbf{l}^X \in \mathcal{L}^X$, we can identify a corresponding conserved quantity $(\mathbf{l}^X)^T \mathbf{x}$:

$$\frac{d(\mathbf{l}^X)^T \mathbf{x}}{dt} = (\mathbf{l}^X)^T \mathbb{S}^X \mathbf{J} = \mathbf{0}. \quad (11)$$

Although some conservation laws are violated in the presence of chemostatted species, the entire set \mathcal{L} remains a valuable tool for identifying permissible reactions in a given CRN. These are reactions that can happen in principle, since they are compatible with the conservation laws determined by \mathbb{S} , even if they are not possible in the CRN under investigation. Analogously to the concept of EFMs, we introduce the set of elementary conservation laws (ECLs). Each ECL \mathbf{r} has a minimal and irreducible support. Thus, each feasible reaction not present in a given open CRN, $\hat{\rho}$, is represented by stoichiometric columns $\mathbb{S}_{\hat{\rho}}$, satisfying $\mathbf{r}^T \mathbb{S}_{\hat{\rho}} = 0$ for all \mathbf{r} . We name “reaction space”, \mathcal{R} , the set of all possible reactions in a CRN that are compatible with the conservation laws associated with the full stoichiometric matrix \mathbb{S} .

The reaction space will be the foundational point to determine the thermodynamic space of general CRN. In fact, the introduction of a fictitious test reaction will allow us to bound the range of concentrations by exploring also chemical transitions that are possible (not present) in a CRN, i.e., belonging to \mathcal{R} .

D. Global thermodynamics of CRNs - Cycle affinity and equilibrium condition

The thermodynamic properties of CRNs are fundamentally characterized by the LDB condition, Eq. (6). These condition relates the degree of irreversibility of reaction fluxes to changes in Gibbs free energy, whose reverse is the affinity of reaction, and represents a local relationship. Additionally, CRNs have global topological properties that are captured by their EFMs. By combining EFMs and thermodynamic features of individual reactions, we can have a quantification of the thermodynamics of a CRN at a global level.

For any given EFM, $\mathbf{e} \in \mathcal{E}$, we can evaluate a cycle

affinity as follows:

$$A_{\mathbf{e}} = \mathbf{e}^T \mathbf{A} = \underbrace{\mathbf{e}^T \mathbf{A}^X}_{=0} + \underbrace{\mathbf{e}^T \mathbf{A}^Y}_{=-\Delta_{\mathbf{e}} G_Y} = A_{\mathbf{e}}^Y. \quad (12)$$

which is the net affinity considering all reactions participating to \mathbf{e} . Notice that Eq. (12) holds for both stationary and non-stationary states [39, 40]. By definition, proceeding along an EFM does not alter internal species concentrations, hence $\mathbf{e}^T \mathbf{A}^X = 0$. The cycle affinity arises solely from concentration changes of chemostatted species, as they are compensated by external fluxes (see Eq. (4)). Consequently, the cycle affinity equals the negative Gibbs free energy change in the chemical reservoirs performing the corresponding reaction cycle, i.e., $A_{\mathbf{e}}^Y = -\Delta_{\mathbf{e}} G_Y$. This is a sheer structural property of the CRN and is independent of the concentrations of the internal species [35].

It is crucial to understand how this property reflects the equilibrium and non-equilibrium conditions of a CRN. At equilibrium, all net fluxes vanish, i.e., $\mathbf{J}^{\text{eq}} = \mathbf{0}$, and accordingly, all affinities are equal to zero, i.e., $\mathbf{A}^{\text{eq}} = \mathbf{0}$. This means that, by using the definition of affinity vector in Eq. (7), the equilibrium condition equivalently requires $\mathbb{S}^T \boldsymbol{\mu}^{\text{eq}} = \mathbf{0}$. Closed CRNs always reach equilibrium. On the contrary, open CRNs often cannot equilibrate, as $\mathbf{A}^{\text{eq}} = \mathbf{0}$ is generally incompatible with the cycle affinity condition in Eq. (12). Indeed, the presence of chemostatted species typically maintains open CRNs out-of-equilibrium, potentially leading to the emergence of a variety of attractors (e.g., fixed points, limit cycles, strange attractors) depending on the kinetics. However, if all chemostatted species are maintained at their equilibrium concentrations, i.e., $\mathbf{e}^T \mathbf{A}^Y = 0$ for each EFM \mathbf{e} , the open CRN will relax to equilibrium [25, 41].

III. UNIVERSAL THERMODYNAMIC BOUNDS FOR CHEMICAL REACTION NETWORKS

A. Thermodynamic accessible region for affinities

Cycle affinities along EFMs offer a global perspective on the thermodynamic features of CRNs and quantify their deviation from equilibrium condition. However, the steady-state value of all reaction affinities throughout the network remains challenging to determine. In fact, the affinity distribution stems from the presence of external chemostatted species and its determination requires solving the system with detailed kinetics. The inherent non-linearity of most of the non-equilibrium CRNs often precludes analytical solutions, making necessary the use of numerical methods to characterize the thermodynamics of non-equilibrium stationary states. Despite the dependence of the affinity distribution on kinetic details, here we demonstrate that thermodynamic bounds on reaction affinities, that are local quantities, can be established using only thermodynamic and topological properties of the CRN, i.e., global properties. This approach provides

valuable insights into the behavior of non-equilibrium systems without requiring complete knowledge of their kinetics. Moreover, it offers a promising perspective on the understanding of how - and within which limits - thermodynamic drivings can effectively enhance (or reduce) reaction affinities, an effect shown to be relevant in various chemical systems [14, 42, 43].

To derive these universal thermodynamic bounds, we begin by assuming the existence of (one or multiple) steady-state solutions with non-zero species concentrations for the CRN, represented by fixed points of Eq. (4). We recall from Sec. (IIB) that, since J^{ss} admits a conformal decomposition, each non-zero flux along an edge in the CRN (i.e., each reaction) must be contained in at least one conformal EFM. Moreover, for a given reaction ρ , the component of the flux J_ρ has the same sign as the affinity $A_\rho = RT \ln(J_\rho^+/J_\rho^-)$. Thus, conformal EFMs are also aligned with the steady-state affinity vector \mathbf{A}^{ss} . Consider then a reaction ρ' , and let \mathbf{e}^* denote the conformal EFM to which ρ' belongs (i.e. $\mathbf{e}_{\rho'}^* \neq 0$). We can rewrite Eq. (12) to isolate the affinity of the ρ' -th reaction:

$$e_{\rho'}^* A_{\rho'}^{\text{ss}} = A_{\mathbf{e}^*}^Y - \sum_{\rho \neq \rho'} e_{\rho}^* A_{\rho}^{\text{ss}}. \quad (13)$$

Since \mathbf{e}^* is conformal to \mathbf{A}^{ss} , all the terms in the summation are positive, so that:

$$0 < e_{\rho'}^* A_{\rho'}^{\text{ss}} < A_{\mathbf{e}^*}^Y. \quad (14)$$

This bound lies on the knowledge of the conformal EFM which, in turn, requires the knowledge of the steady-state flux and, as such, the entire kinetics. To proceed further and derive a sheer thermodynamic bound, we maximize over all EFMs that contains the reaction ρ' in the same direction as the conformal EFM \mathbf{e}^* , i.e., all \mathbf{e} such that $\text{sgn}(e_{\rho'}) = \text{sgn}(e_{\rho'}^*)$ or, equivalently, $e_{\rho'} e_{\rho'}^* > 0$. Thus:

$$0 < \text{sgn}(e_{\rho'}^*) A_{\rho'}^{\text{ss}} < \frac{A_{\mathbf{e}^*}^Y}{|e_{\rho'}^*|} \leq \max_{\mathbf{e}: e_{\rho'} e_{\rho'}^* > 0} \frac{A_{\mathbf{e}}^Y}{|e_{\rho'}|}. \quad (15)$$

By defining $\mathcal{E}_{\rho'}^{+(-)}$ as the set of all EFMs whose component $e_{\rho'} > 0 (< 0)$, we have:

$$0 < A_{\rho'}^{\text{ss}} < \max_{\mathcal{E}_{\rho'}^+} \frac{A_{\mathbf{e}}^Y}{e_{\rho'}} \quad \text{if } e_{\rho'}^* > 0 \quad (16)$$

$$\min_{\mathcal{E}_{\rho'}^-} \frac{A_{\mathbf{e}}^Y}{e_{\rho'}} < A_{\rho'}^{\text{ss}} < 0 \quad \text{if } e_{\rho'}^* < 0 \quad (17)$$

where we used the fact that, when $e_{\rho'}^* < 0$, the right-side of Eq. (15) becomes equal to $\max_{\mathcal{E}_{\rho'}^-} (A_{\mathbf{e}}^Y/|e_{\rho'}|) = \max_{\mathcal{E}_{\rho'}^-} (-A_{\mathbf{e}}^Y/e_{\rho'}) = -\min_{\mathcal{E}_{\rho'}^-} (A_{\mathbf{e}}^Y/e_{\rho'})$, by exploiting the negativity of $e_{\rho'}$. Plugging together Eqs. (16) and (17), for an arbitrary ρ , we finally have:

$$\min \left(0, \min_{\mathcal{E}_{\rho}^-} \frac{A_{\mathbf{e}}^Y}{e_{\rho}} \right) \leq A_{\rho}^{\text{ss}} \leq \max \left(0, \max_{\mathcal{E}_{\rho}^+} \frac{A_{\mathbf{e}}^Y}{e_{\rho}} \right). \quad (18)$$

Here, we included the equal sign on both inequalities by noting that, at equilibrium, equalities should hold. Hence, although the derivation has been carried out for non-equilibrium systems, it can be readily extended to equilibrium ones. In fact, in a system without non-equilibrium drivings induced by chemostatted species, all cycle affinities vanish ($A_{\mathbf{e}}^Y = 0$ for all cycles). This condition ensures that, at stationarity, all reaction affinities also vanish ($A_{\rho}^{\text{ss}} = 0$ for all reactions), thus the steady state is an equilibrium state and the equalities hold. In the presence of non-equilibrium driving, however, Eq. (18) uncovers the thermodynamic limits of the deviation from equilibrium for each reaction affinity, solely based on global out-of-equilibrium properties. We remark here that the inequality in Eq. (18) turns into an equality also when the presence of non-equilibrium driving gives a net zero flux and, as such, zero affinity. The system effectively behaves as an equilibrium system and equalities are restored as discussed above. A crucial observation is that this formulation does not rely on the knowledge of the EFM conformal to the steady-state flux and holds for any reaction in the CRN.

Furthermore, the affinity of a reaction ρ can be decomposed into contributions from internal and external species, i.e., $A_{\rho} = A_{\rho}^{X,\text{ss}} + A_{\rho}^Y$ (see Eq. (8)). By moving A_{ρ}^Y to the right side of Eq. (18), we obtain an upper bound on the affinity of internal species:

$$A_{\rho}^{X,\text{ss}} \leq \max \left(-A_{\rho}^Y, \max_{\mathcal{E}_{\rho}^+} \frac{A_{\mathbf{e}}^Y - e_{\rho} A_{\rho}^Y}{e_{\rho}} \right) \\ = \max_{\Pi_{\rho}^X} A_{\pi_{\rho}^X}^Y \quad (19)$$

Here, we define Π_{ρ}^X as the set of all reaction pathways constructed through EFMs that convert the internal species X from the right side of reaction ρ to its left side, as indicated by the minus sign, where the reaction ρ itself has been eliminated from each pathway. Each element of Π_{ρ}^X is indicated by π_{ρ}^X . Analogously, Π_{ρ}^+ contains pathways that convert X from the left to the right side of ρ . The last equality in Eq. (19) can be easily understood by noting that all EFMs such that $e_{\rho} > 0$, i.e., those in \mathcal{E}_{ρ}^+ , convert X from its value on the right to the left side of ρ when ρ itself is eliminated. The affinity of a pathway constructed from $\mathbf{e} \in \mathcal{E}_{\rho}^+$ is $A_{\mathbf{e}}^Y/e_{\rho} - A_{\rho}^Y$, where we divided by e_{ρ} since there might be more conversion of X through ρ in some EFMs. Also, before the elimination of ρ , this set of pathways that we named Π_{ρ}^X contains ρ itself in the backward direction. After elimination, the resulting affinity is simply $-A_{\rho}^Y$. From these observations, Eq. (19) immediately follows. An analogous procedure yields to a lower bound on $A_{\rho}^{X,\text{ss}}$.

1. Thermodynamic bounds on effective affinities

Despite its generality, Eq. (18) applies only to reaction affinity that are present in the CRN. However, it is

possible to surpass this limitation and derive upper and lower thermodynamic bounds for the effective affinity of reactions that are not present in the original CRN, while being in principle compatible with it.

Recalling that the reaction space is defined as the space orthogonal to the conservation laws of the original stoichiometric matrix, it contains all possible reactions that are in principle compatible with the CRN under study. We introduce the idea of a “chemical probe”, a test reaction that belongs to the reaction space but not to the original network. The resulting extended stoichiometric matrix is then $\tilde{S} = [S, \hat{S}_\rho]$, where the newly introduced reaction is represented by the column \hat{S}_ρ . We assume that $\hat{\rho}$ proceeds so slowly that its net flux is negligible, i.e., $J_{\hat{\rho}} \simeq 0$. However, it still maintains a finite affinity $A_{\hat{\rho}} = RT \ln[J_{\hat{\rho}}^+ / J_{\hat{\rho}}^-]$, which depends on the chemical potentials of the species involved in the reaction. To determine the affinity associated with this test reaction $\hat{\rho}$, we consider one conformal EFM containing $\hat{\rho}$, e^F . For this, according to the previous relationship, we have:

$$\text{sgn}(e_{\hat{\rho}}^F) A_{\hat{\rho}}^{\text{ss}} < \max_{\mathcal{E}_{\hat{\rho}}^+} \frac{A_e^Y}{|e_{\hat{\rho}}|}. \quad (20)$$

Since, by construction, the chemical probe alter only infinitesimally the dynamics of the original system, there should exist another EFM that pass through $\hat{\rho}$ along the same direction, but is anti-conformal to the steady-state flux of the original CRN. This property comes directly from the fact that we know that the original CRN (without the probe) admits a non-equilibrium steady state and, as such, necessarily supports the existence of closed fluxes. Let e^B be this EFM, we have:

$$\text{sgn}(e_{\hat{\rho}}^B) A_{\hat{\rho}}^{\text{ss}} > \frac{A_{e^B}^Y}{|e_{\hat{\rho}}^B|} \geq \min_{\mathcal{E}_{\hat{\rho}}^+} \frac{A_e^Y}{|e_{\hat{\rho}}|}, \quad (21)$$

by using the anti-conformality along all reactions but $\hat{\rho}$. We can arbitrarily fix the sign of $e_{\hat{\rho}}^F$ to be positive and, by construction, the sign of $e_{\hat{\rho}}^B$ will be positive as well. Thus, by putting together Eqs. (20) and (21), we have:

$$\min_{\mathcal{E}_{\hat{\rho}}^-} \frac{A_e^Y}{e_{\hat{\rho}}} \leq A_{\hat{\rho}}^{\text{ss}} \leq \max_{\mathcal{E}_{\hat{\rho}}^+} \frac{A_e^Y}{e_{\hat{\rho}}}, \quad (22)$$

where we used that equalities describe the equilibrium condition, as before, and that $\min_{\mathcal{E}_{\hat{\rho}}^+} A_e^Y / e_{\hat{\rho}} = \min_{\mathcal{E}_{\hat{\rho}}^-} A_e^Y / e_{\hat{\rho}}$, since both affinities and $e_{\hat{\rho}}$ change sign. It is immediate to check that, if $\text{sgn}(e_{\hat{\rho}}^F) = \text{sgn}(e_{\hat{\rho}}^B) < 0$, this sandwich inequality still holds. Crucially, Eq. (22) provides a tighter bound with respect to Eq. (18), since we used the additional information characterizing the chemical probe. This sandwich inequality holds for any reaction belonging to the reaction space and determine the thermodynamic limits of any effective affinity, given an energy budget determining non-equilibrium conditions. Therefore, Eqs. (18) and (22) constitute the first main result of this study.

By splitting the affinity into the contribution given by internal and external species, we can rewrite the upper bound as follows:

$$A_{\hat{\rho}}^{X,\text{ss}} \leq \max_{\mathcal{E}_{\hat{\rho}}^+} \frac{A_e^Y - e_{\hat{\rho}} A_{\hat{\rho}}^Y}{e_{\hat{\rho}}} = \max_{\Pi_{\hat{\rho}}^X} A_{\pi_{\hat{\rho}}^X}^Y \quad (23)$$

and the same holds for the lower bound. There is one main difference between this expression, valid for the affinity of a reaction not present in the original CRN, and the one presented in Eq. (19). In the first case, the term given by the the direct reaction $\hat{\rho}$ does not appear and, as such, the pathways converting X from the right to the left of $\hat{\rho}$ have to be considered in the original CRN. This property is perfectly consistent with the notation here introduced and with the fact that this chemical probe is only a mathematical tool to investigate the system devoid of any physical information. As a final comment, such a chemical probe can be considered analogous to a voltmeter in an electric circuit. Both measure potential differences with minimal disturbance: the probe is introduced gradually, resulting in an infinitely slow edge of the network, while an ideal voltmeter has infinite resistance, leading to infinitesimal flux. As such, the probe uses its vanishing chemical flux to gauge the chemical potential difference between network nodes, similarly to how a voltmeter measures voltage. As we will see in the next section, this approach will be crucial to determine the whole thermodynamic space of a CRN.

B. Thermodynamic space of CRNs - Accessible region for species concentrations

From the bounds on reaction affinities, we can derive upper and lower bounds on species concentrations. These limits determine the accessible region for each chemical species given the CRN’s energy budget. We name this region “thermodynamic space”. The same concept has been already introduced in [20], where it has been found for pseudo-unimolecular CRNs. Also, the idea of a space which is thermodynamically accessible given the external non-equilibrium constraints is of fundamental importance in various contexts, such as metabolic networks [38], signal amplification [33], and self-assembly [44].

Although concentrations are not explicit thermodynamic quantities, they are encoded in chemical potentials. We recall that affinities can also be expressed by means of chemical potentials. By specifying Eq. (7) for $A_{\rho}^{X,\text{ss}}$ and $A_{\pi_{\rho}^X}^Y$, we have:

$$\begin{aligned} A_{\rho}^{X,\text{ss}} &= -\Delta_{\rho} G_X^{\circ} - RT \sum_i S_{i\rho}^X \ln x_i^{\text{ss}}, \\ A_{\pi_{\rho}^X}^Y &= -\Delta_{\pi_{\rho}^X} G_Y, \end{aligned} \quad (24)$$

where $\Delta_{\rho} G_X^{\circ}$ indicates the standard Gibbs free-energy change of X along ρ , and $\Delta_{\pi_{\rho}^X} G_Y$ the Gibbs free-energy

change of Y along the reaction pathway $\pi_{\rho^-}^X$. By combining Eqs. (19) and (24), and employing the duality of affinity, i.e., $A_{\pi_{\rho^-}^X}^Y = -A_{\pi_{\rho^+}^X}^Y$ for any $\pi_{\rho^\pm}^X$ so that:

$$\max_{\pi_{\rho^-}^X} A_{\pi_{\rho^-}^X}^Y = -\min_{\pi_{\rho^+}^X} A_{\pi_{\rho^+}^X}^Y, \quad (25)$$

we obtain bounds on the internal concentrations involved in the reaction ρ :

$$\prod_i (x_i^{ss})^{\mathbb{S}_{i\rho}^X} \geq \min_{\pi_{\rho^+}^X} \exp \left[-\underbrace{\frac{\Delta_\rho G_X^\circ + \Delta_{\pi_{\rho^+}^X} G_Y}{RT}}_{K_{\pi_{\rho^+}^X}} \right] \equiv K_{\pi_{\rho^+}^X}^{\min} \quad (26)$$

Here, $K_{\pi_{\rho^+}^X}$ is the effective equilibrium constant for a reaction pathway converting chemical species between the two sides of reaction ρ . Indeed, if the CRN only had one pathway, say $\pi_{\rho^+}^X$, the system would reach equilibrium and the product of concentrations of species involved in ρ with stoichiometric exponents, $\prod_i (x_i^{ss})^{\mathbb{S}_{i\rho}^X}$, would be exactly equal to $K_{\pi_{\rho^+}^X}$. As indicated in Eq. (26), the concentrations are lower bounded by the equilibrium constant minimized over all pathways. Following the same procedure, we can derive also an upper bound, resulting in the following range of accessible concentrations for all species involved in ρ :

$$K_{\pi_{\rho^+}^X}^{\min} \leq \prod_i (x_i^{ss})^{\mathbb{S}_{i\rho}^X} \leq K_{\pi_{\rho^+}^X}^{\max} \quad (27)$$

The bounds in Eq. (27) have been derived for the concentration of species connected by a reaction ρ . However, starting from Eq. (23), we can see that analogous bounds hold for any species connected by a fictitious reaction $\hat{\rho}$ which is compatible with the conservation laws, i.e., it belongs to the reaction space of the CRN. These bounds are identical to Eq. (27) by replacing ρ with $\hat{\rho}$ and the pathways have to be constructed from the original CRN (as the chemical probe never existed), consistently with the physical content of the system. Thus, Eq. (27) constitutes the second main result of this study.

Let us investigate the difference between equilibrium and non-equilibrium conditions and the information that the thermodynamic space can provide on the system. At thermodynamic equilibrium, all driving forces vanish and, as such, the equilibrium constant becomes identical for all pathways and equal to the standard Gibbs free-energy difference of internal species, as expected. Consequently, Eq. (27) becomes an equality on both sides, thus the stationary value of all concentrations converges to a unique one dictated by their free energies and the conservation laws of the CRN. In contrast, out-of-equilibrium CRNs exhibit a range of feasible stationary concentrations. This constitutes a subspace of the whole phase-space of species concentrations, and it depends on the global non-equilibrium thermodynamic properties

of the network. In general, a non-zero thermodynamic space enables complex dynamics and is a prerequisite for complex behaviors such as free-energy transduction, bi-stability, pattern formation, and kinetically responsive states. The thermodynamic space, encoded in the bounds of Eq. (27), quantifies the intimate relationship between non-equilibrium conditions and emergent complexity in any CRN, therefore providing a measure of potential functional diversity and efficiency of complex biochemical processes.

C. Connections to previous results

In this work, we derived two main results: the thermodynamic constraints on reaction affinity at stationary state in terms of cycle affinities, i.e., Eqs. (18) and (22)), and the bounds on species concentrations in terms of (pseudo-)equilibrium constants, i.e., Eq. (27), that define the thermodynamic space of the CRN. To our knowledge, these bounds for generic CRNs are novel, although similar bounds have been previously established for special cases of CRN such as linear and catalytic CRNs.

In linear and catalytic CRNs, the columns of stoichiometric matrix entries are restricted to have only one +1 and one -1 for internal species, effectively rendering the CRN a graph rather than a hypergraph. For such graph networks, a simple conservation law applies $\mathbf{r} = \mathbf{1}$, i.e., $\sum_i x_i = \text{constant}$. Moreover, the matrix-tree theorem allows the representation of steady-state solutions through spanning trees, facilitating the derivation of thermodynamic bounds on steady-state observables. Previous results, primarily discussed in the context of stochastic thermodynamics, expressed bounds in terms of probability ratios. These probabilities can be interpreted as normalized concentrations of internal species with respect to the conservation law, i.e., $p_i = x_i / \sum_i x_i$. This formulation allowed for a direct connection between deterministic and stochastic descriptions of the system:

$$K_{\pi_{X_i \rightarrow X_{i'}}}^{\min} \leq \frac{p_{i'}^{ss}}{p_i^{ss}} \leq K_{\pi_{X_i \rightarrow X_{i'}}}^{\max}, \quad (28)$$

which can directly come from Eq. (27) by choosing a chemical probe $X_i \rightleftharpoons X_{i'}$ such that $\mathbb{S}_{i\hat{\rho}} = -1$ and $\mathbb{S}_{i'\hat{\rho}} = 1$. An equivalent form of the above result was first discovered by Maes and Netočný for linear networks [31], in which the upper and lower bounds were expressed using the heat dissipation through minimal and maximum dissipation pathways, i.e. rewriting the (pseudo-)equilibrium constants in terms of free energy changes. Lin has derived a similar result by drawing an analogy between electric circuits and linear CRNs [45]. Subsequently, our previous work demonstrated that these bounds also hold for non-linear catalytic networks [20], where catalytic effects do not change the entries of the stoichiometric matrix and maintain the CRN as an effective graph instead of a hypergraph. Furthermore, Liang and Pigolotti provided additional proof based on

the propagator instead of matrix-tree theorem for the same bound on linear networks and extended the analysis to derive bounds on the asymmetry of steady-state semi-fluxes in graph networks [46]:

$$\left| \ln \frac{J_\rho^+}{J_\rho^-} \right| \leq \max_{e \ni \rho} A_e^Y / RT. \quad (29)$$

This result can be seen as a special case of Eq. (18) for linear CRNs, expressing the ratio of forward and backward semi-fluxes using the LDB condition, Eq. (6).

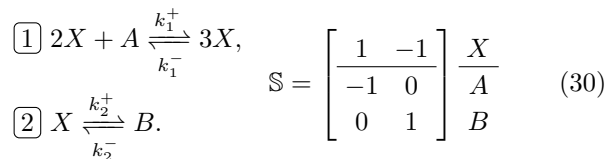
Ultimately, we remark that the result presented here encompasses all previous work, generalizing their findings (both on affinities and species concentrations) to general CRNs. Such extension constitutes the first mathematical derivation of the range of operations of chemical systems. Therefore, it can unravel general properties of a variety of different systems and lead to universal answers in multiple fields, ranging from proofreading to the origin of life, where hitherto only solutions for specific systems have been obtained.

IV. APPLICATIONS

A. Application 1: Schlögl model for bistability

Out-of-equilibrium open CRNs may exhibit emergent complex phenomena, such as multi-stability, where the reaction dynamics in Eq. (4) exhibits multiple stable fixed points. The Schlögl model, a minimal model for multi-stability, can sustain two stable modes at stationarity within specific parameter ranges [8, 47]. Analyzing this feature in such a paradigmatic model is crucial for understanding the role of non-equilibrium thermodynamic driving in constraining and shaping the bi-stable nature of chemical reaction systems.

The Schlögl model is defined by the following reactions and stoichiometric matrix:



where X is an internal species, and A and B are two chemostatted external species. These reactions can be represented by the reaction hypergraph shown in Fig. 1(a). The network contains a single EFM $e = [1, 1]$, as shown in Fig. 1(b). Along this EFM, one external species (A) is converted into an external species (B), with an associated free-energy change $\Delta_e G = \mu_B - \mu_A = \mu_B^\circ - \mu_A^\circ + RT \ln(b/a)$. Consequently, its cycle affinity is $A_e = -\Delta_e G$. Applying Eq. (18), we derive bounds on the affinities of both reactions for the internal species:

$$0 \leq A_{\rho=1}^{\text{ss}} \leq \mu_A - \mu_B, \quad 0 \leq A_{\rho=2}^{\text{ss}} \leq \mu_A - \mu_B. \quad (31)$$

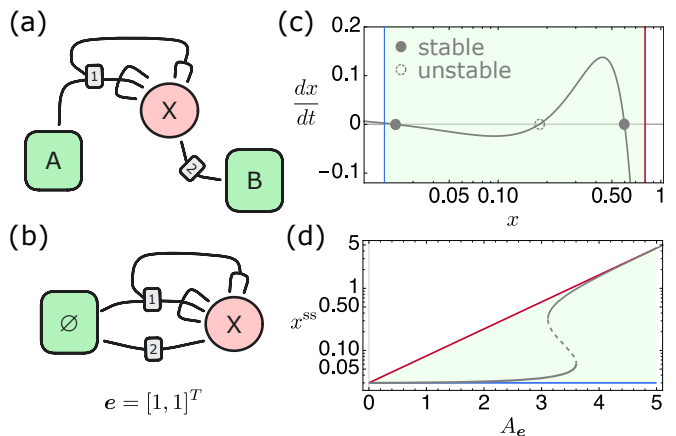


FIG. 1. Thermodynamic space of the Schlögl model. (a) Reaction hypergraph of the Schlögl model with an internal species X and two chemostatted external species A and B . (b) The EFM of the Schlögl model, in which the internal species X is created from the environment \emptyset and then degraded into it respectively through reactions 1 and 2. (c) Time derivative of the concentration of X as a function of $x = [X]$. Fixed points (zeros of the derivative) are constrained within the thermodynamic space (green-shaded region). (d) Bifurcation diagram with cycle affinity $A_e = \mu_A - \mu_B$ as the control parameter. Stable (solid lines) and unstable (dashed lines) solutions are bounded by the thermodynamic space (green-shaded region). Red and blue lines in (c) and (d) represent the lower and upper bound of the thermodynamic space, respectively, as derived from Eq. (32).

To constrain the concentration of the internal species, we apply Eq. (27) for all species involved in the first reaction (the same would also, in this case, considering the second reaction, since we can only bound X as internal species). We identify the minimum and maximum equilibrium constants for the transformation from chemostatted species to internal species, $\emptyset \rightarrow X$, which can be achieved through two pathways: $\pi_{\emptyset \rightarrow X}^{(1)} = [1, 0]$ (first reaction) and $\pi_{\emptyset \rightarrow X}^{(2)} = [0, -1]$ (reverse of second reaction). By minimizing and maximizing the equilibrium constants across these pathways, we obtain bounds on the steady-state concentration of the internal species X :

$$\exp \left[-\frac{\mu_X^\circ - \mu_B}{RT} \right] \leq x^{\text{ss}} \leq \exp \left[-\frac{\mu_X^\circ - \mu_A}{RT} \right]. \quad (32)$$

The range of steady-state concentration bounds the fixed points of the reaction dynamics. In Fig. 1(c), we show that this region contains both stable and unstable fixed points, while in Fig. 1(d) we bound the bifurcation diagram for different values of the cycle affinity $A_e = \mu_A - \mu_B$. The lower and upper bound of Eq. (32), indicated by red and blue lines in Fig. 1, can be asymptotically approached in the timescale separation limit. In fact, the system reaches the upper bound when the first reaction proceeds much faster than the second, allowing it to reach a quasi-equilibrium state. Conversely, the lower bound is approached when the second reac-

tion is significantly faster, dominating the system dynamics. This timescale separation principle provides insight into how kinetic parameters can drive the system towards different extremes within its thermodynamically allowed range, highlighting the interplay between thermodynamic constraints and kinetic factors in determining steady-state concentrations.

The nontrivial bistability in this reaction system emerges from the high-order autocatalytic nature of the first reaction. This autocatalysis modulates reaction rates based on the concentration of species X , leading to two stable fixed points approaching the upper and lower bounds of the thermodynamic space defined by Eq. (32). These bounds effectively constrain the range of stable fixed points. In equilibrium systems, where $\Delta_e G = \mu_B - \mu_A = 0$, the lower and upper bounds converge, collapsing the thermodynamic space and precluding bistable solutions. This collapse elucidates the necessity of non-equilibrium driving forces for the emergence of complex behaviors in chemical reaction networks (CRNs), even in simple models.

While we present a minimal model for multistability in CRNs, our thermodynamic constraints apply to arbitrary CRNs and can be potentially extended to complex biochemical processes in cellular systems, illuminating bistable modes in gene regulation or other biological functions whose robustness resides in the presence of multistability. These thermodynamic constraints demonstrate how complex behaviors emerge within physical limits. The interplay between nonlinear kinetics and thermodynamic constraints underscores the importance of thermodynamic analysis in predicting CRN dynamics, even without detailed kinetic information, providing a tool for understanding thermodynamic prerequisites for complex behaviors in chemical and biological systems.

B. Application 2: Self-Assembly

In this section, we study a minimal self-assembly model to demonstrate the application of our thermodynamic constraints to CRNs that also encompass the presence of molecular complexes. The proposed model is composed of three reactions: a fuel-to-waste conversion driving the dimer formation, a spontaneous association of a dimer and a monomer to form a trimer, and the spontaneous disassembly from a trimer to three monomers. Here, the fuel F and the waste W are treated as chemostatted external species, keeping the system out of equilibrium. The detailed reaction scheme is illustrated in Eq. (33), together with the stoichiometric matrix, while the corresponding reaction hypergraph is represented in Fig. 2a

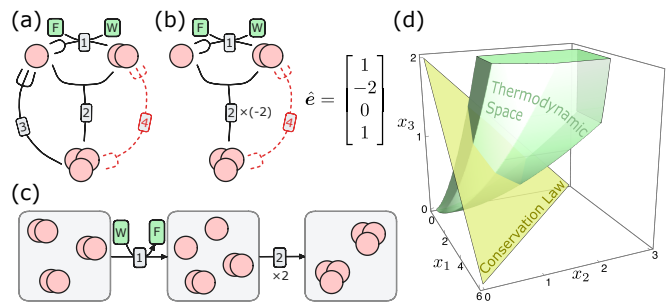
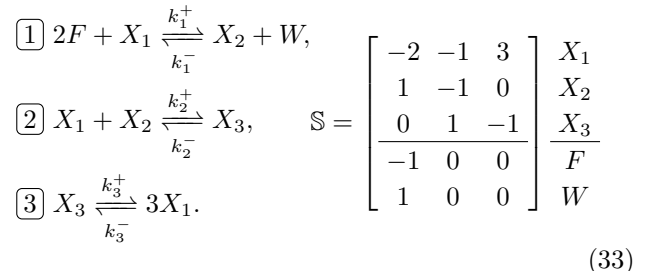


FIG. 2. (a) Reaction hypergraph with three internal species, two external species (F , W), and a chemical probe (dashed red). (b) Elementary flux mode (EFM) including the chemical probe, with vector representation \hat{e} . (c) A sequence of reactions from the EFM, converting species from left to right of the probe. (d) Thermodynamic space (green) intersecting with conservation law plane (yellow), defining possible steady-state concentrations of internal species.

with black hyperedges.



For this self-assembly CRN, there is one EFM, $e = [1, 1, 1]^T$ in the reaction hypergraph and its cycle affinity $A_{e_1} = \mu_F - \mu_W = \Delta\mu > 0$ since it stems from the fuel-to-waste driven dimer formation. We further assume that this chemical potential difference is strictly positive in the model. This cycle affinity bounds the affinity of all three reactions by means of Eq. (18)

$$0 \leq A_\rho^{\text{ss}} \leq \Delta\mu, \text{ for } \rho = 1, 2, 3. \quad (34)$$

Using Eq. (27), we can also bound the concentration ratios of internal species involved in these three reactions

$$\begin{aligned}
 e^{-\frac{\mu_2^\circ - 2\mu_1^\circ}{RT}} &\leq \frac{x_2^{\text{ss}}}{(x_1^{\text{ss}})^2} \leq e^{-\frac{\mu_2^\circ - 2\mu_1^\circ - \Delta\mu}{RT}} \\
 e^{-\frac{\mu_3^\circ - \mu_2^\circ - \mu_1^\circ + \Delta\mu}{RT}} &\leq \frac{x_3^{\text{ss}}}{x_1^{\text{ss}} x_2^{\text{ss}}} \leq e^{-\frac{\mu_3^\circ - \mu_2^\circ - \mu_1^\circ}{RT}} \\
 e^{-\frac{\mu_3^\circ - 3\mu_1^\circ + \Delta\mu}{RT}} &\leq \frac{(x_1^{\text{ss}})^3}{x_3^{\text{ss}}} \leq e^{-\frac{\mu_3^\circ - 3\mu_1^\circ}{RT}}
 \end{aligned} \quad (35)$$

where we use μ_1° , μ_2° , and μ_3° to denote the standard chemical potential of internal species X_1 , X_2 and X_3 , respectively. The constraints on concentrations define the thermodynamic space illustrated in Fig. 2d.

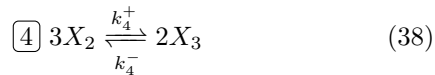
From the right nullspace of $(\mathbb{S}_X)^T$, we can extract one elementary conservation law (ECL)

$$r = [1, 2, 3]^T \quad (36)$$

such that we have the following conserved quantity

$$x_1 + 2x_2 + 3x_3 = \text{constant}. \quad (37)$$

This conservation law allows us to find one additional allowed reaction



which belongs to the reaction space but it is not present in the original CRN. Thus, we add a chemical probe to the CRN that represents this extra reaction, as indicated by the number 4 and the red dashed hyperedge in Fig. 2a-b. This procedure corresponds to the addition of a new stoichiometric column $\hat{S}_\rho = [0, -3, 2]^T$ which is, by definition, orthogonal to the conservation law by definition, i.e., $\mathbf{r}^T \hat{S}_\rho = 0$. There is only one EFM in the extended stoichiometric matrix $\tilde{S} = [S, \hat{S}_\rho]$ that encloses the extra reaction given by the chemical probe:

$$\hat{e} = [1, -2, 0, 1]^T \quad (39)$$

From this, we can find the bounds on species concentrations on the two sides of reaction 4 again by using Eq. (27), i.e. by finding the pathways from \hat{e} that convert the dimer into the trimer, and evaluating their corresponding (pseudo-)equilibrium constants:

$$e^{-\frac{2\mu_3^{\circ} - 3\mu_2^{\circ} + \Delta\mu}{RT}} \leq \frac{(x_3^{\text{ss}})^2}{(x_2^{\text{ss}})^3} \leq e^{-\frac{2\mu_3^{\circ} - 3\mu_2^{\circ}}{RT}}. \quad (40)$$

Analogously, we can bound the effective affinity of this additional reaction by means of Eq. (22):

$$-\Delta\mu \leq A_\rho^{\text{ss}} \leq 0 \quad (41)$$

The simplicity of this self-assembly CRN made us able to show the power of the proposed framework. Because of its potential feasibility to study more interesting scenarios, we are currently employing it to investigate complex self-assembly CRNs.

V. DISCUSSION

In this work, we have derived fundamental thermodynamic constraints on generic CRNs at stationarity, introducing the novel concept of *thermodynamic space* to describe the feasible range of species concentrations compatible with the system's energy budget. Similar bounds can also be obtained for reaction affinities and employed to estimate the limits of effective affinities between any two species in the CRN. Our approach is based on CRN hypergraph geometry and utilizes the novel *chemical probe* technique to study species that are directly linked by an existing reaction. Therefore, it significantly extends and generalizes previous findings on linear and catalytic networks, i.e., pseudo-unimolecular CRNs, to arbitrary network topologies. This generalization is crucial for applications in complex multimolecular CRNs,

such as multi-stationary biochemical networks and self-assembly processes, which are widespread in living systems but their study has fallen short of a comprehensive thermodynamic analysis. We believe that the results we introduced will be crucial to characterize CRNs starting solely from global thermodynamic properties without the need of relying on simplified (often unrealistic) models.

We demonstrate our framework's applicability through two examples, the Schlögl model for bistability and a simple self-assembly amplification. These case studies illustrate how our bounds elucidate thermodynamic prerequisites for complex behaviors, providing insights into the emergence of multistability (and eventually pattern formation) in biological systems. Our approach bridges concepts from non-equilibrium thermodynamics, network theory, and systems biology, offering a powerful interdisciplinary tool for analyzing living systems.

The generality of our framework opens avenues for diverse applications beyond those explored here. For instance, it could be extended to bound responses to kinetic parameter perturbations in multi-molecular CRNs, building upon previous results for linear systems [29]. Our approach also has the potential to generalize studies on the information propagation in molecular templating networks without making pseudo-unimolecular constraints [48, 49]. Furthermore, the idea of building a thermodynamic space has been previously discussed in the context of metabolic networks as a constrained optimization problem [50]. Our results provide the exact form of such space, setting foundational building blocks to characterize the operation range of the metabolic activity of any CRN from thermodynamic considerations on free-energies and external chemostatted species. Future works could also explore applications to other nonlinear phenomena in biochemical systems, such as biochemical oscillations. An exciting direction would be to investigate thermodynamic bounds on various attractor types (e.g., limit cycles, strange attractors), potentially allowing to extend the concept of thermodynamic space beyond stationary states. This could provide insights into the thermodynamic requirements for complex dynamical behaviors in living systems, such as circadian rhythms and calcium oscillations.

In conclusion, this work provides a general framework for analyzing non-equilibrium phenomena in biological and synthetic systems, contributing to a deeper understanding of the principles governing complex chemical and biological processes. By establishing fundamental thermodynamic constraints on the operation of chemical reaction networks, our approach offers new perspectives on the design principles of living systems and can potentially guide the development of artificial molecular systems with life-like properties, such as the emergence of information sequences through complex self-assembly processes [51–55]. Ultimately, this work represents a significant step towards a more comprehensive thermodynamic theory of complex, far-from-equilibrium biological and biochemical systems.

ACKNOWLEDGMENTS

S.L. and P.D.L.R. thanks the Swiss National Science Foundation for support under grant 200020_178763. Part

of this work was finished by S.L. and D.M.B during the Frontiers in Non-equilibrium Physics 2024 Workshop at Yukawa Institute for Theoretical Physics, Kyoto University.

-
- [1] X. Fang, K. Kruse, T. Lu, and J. Wang, *Reviews of Modern Physics* **91**, 045004 (2019).
- [2] X. Yang, M. Heinemann, J. Howard, G. Huber, S. Iyer-Biswas, G. Le Treut, M. Lynch, K. L. Montooth, D. J. Needleman, S. Pigolotti, J. Rodenfels, P. Ronceray, S. Shankar, I. Tavassoly, S. Thutupalli, D. V. Titov, J. Wang, and P. J. Foster, *Proceedings of the National Academy of Sciences* **118**, e2026786118 (2021).
- [3] B. Zoller, T. Gregor, and G. Tkačik, *Current Opinion in Systems Biology* **31**, 100435 (2022).
- [4] B. Ø. Palsson, *Systems Biology: Constraint-based Reconstruction and Analysis* (Cambridge University Press, Cambridge, 2015).
- [5] P. R. ten Wolde, N. B. Becker, T. E. Ouldridge, and A. Mugler, *Journal of Statistical Physics* **162**, 1395 (2016).
- [6] F. Wong and J. Gunawardena, *Annual Review of Biophysics* **49**, 199 (2020).
- [7] M. Feinberg, *Foundations of Chemical Reaction Network Theory*, Applied Mathematical Sciences, Vol. 202 (Springer International Publishing, Cham, 2019).
- [8] M. Vellela and H. Qian, *Journal of The Royal Society Interface* **6**, 925 (2009).
- [9] F. Avanzini, G. Falasco, and M. Esposito, *The Journal of Chemical Physics* **151**, 234103 (2019).
- [10] Y. Cao, H. Wang, Q. Ouyang, and Y. Tu, *Nature Physics* **11**, 772 (2015).
- [11] P. Gaspard, *Chaos: An Interdisciplinary Journal of Non-linear Science* **30**, 113103 (2020).
- [12] D. Li, S. Liao, Q. Ouyang, and F. Li, *Physical Review Research* **6**, 033050 (2024).
- [13] G. Li and H. Qian, *Cell Biochemistry and Biophysics* **39**, 45 (2003).
- [14] P. De Los Rios and A. Barducci, *eLife* **3**, e02218 (2014).
- [15] A. V. Dass, T. Georgelin, F. Westall, F. Foucher, P. De Los Rios, D. M. Busiello, S. Liang, and F. Piazza, *Nature Communications* **12**, 2749 (2021).
- [16] X. Guo, T. Tang, M. Duan, L. Zhang, and H. Ge, *iScience* **25**, 104358 (2022).
- [17] D. Hathcock, Q. Yu, B. A. Mello, D. N. Amin, G. L. Hazelbauer, and Y. Tu, *Proceedings of the National Academy of Sciences* **120**, e2303115120 (2023).
- [18] D. Zhang, C. Zhang, Q. Ouyang, and Y. Tu, *Journal of The Royal Society Interface* **20**, 20230276 (2023).
- [19] G. Falasco, R. Rao, and M. Esposito, *Physical Review Letters* **121**, 108301 (2018).
- [20] S. Liang, P. De Los Rios, and D. M. Busiello, *Physical Review Letters* **132**, 228402 (2024).
- [21] F. Brauns, J. Halatek, and E. Frey, *Physical Review X* **10**, 041036 (2020).
- [22] M. Pekař, *Progress in Reaction Kinetics and Mechanism* **30**, 3 (2005).
- [23] H. Qian, D. A. Beard, and S.-d. Liang, *European Journal of Biochemistry* **270**, 415 (2003).
- [24] H. Ge and H. Qian, *Chemical Physics* **472**, 241 (2016), arXiv:1601.03158 [physics].
- [25] R. Rao and M. Esposito, *Physical Review X* **6**, 041064 (2016), arXiv:1602.07257.
- [26] C. Maes, *SciPost Physics Lecture Notes*, 32 (2021).
- [27] M. Polettini and M. Esposito, *The Journal of Chemical Physics* **141**, 024117 (2014), arXiv:1404.1181 [cond-mat, physics:physics, q-bio].
- [28] S. Dal Cengio, V. Lecomte, and M. Polettini, *Physical Review X* **13**, 021040 (2023).
- [29] J. A. Owen, T. R. Gingrich, and J. M. Horowitz, *Physical Review X* **10**, 011066 (2020).
- [30] M. Bilancioni and M. Esposito, “Elementary Flux Modes as CRN Gears for Free Energy Transduction,” (2024), arXiv:2405.17960 [cond-mat, q-bio].
- [31] C. Maes and K. Netočný, *Annales Henri Poincaré* **14**, 1193 (2013).
- [32] U. Çetiner and J. Gunawardena, *Physical Review E* **106**, 064128 (2022).
- [33] E. Arunachalam and M. M. Lin, “Information gain limit of molecular computation,” (2024), arXiv:2311.15378 [physics].
- [34] T. L. Hill, *Free Energy Transduction and Biochemical Cycle Kinetics* (Springer, New York, NY, 1989).
- [35] J. Schnakenberg, *Reviews of Modern Physics* **48**, 571 (1976).
- [36] S. Klamt, U.-U. Haus, and F. Theis, *PLoS Computational Biology* **5**, e1000385 (2009).
- [37] S. Müller and G. Regensburger, *Frontiers in Genetics* **7** (2016), 10.3389/fgene.2016.00090.
- [38] I. Famili and B. O. Palsson, *Biophysical Journal* **85**, 16 (2003).
- [39] D. A. Beard, E. Babson, E. Curtis, and H. Qian, *Journal of Theoretical Biology* **228**, 327 (2004).
- [40] T. De Donder and P. Van Rysselberghe, *Thermodynamic Theory of Affinity* (Stanford university press, 1936).
- [41] S. Schuster and R. Schuster, *Journal of Mathematical Chemistry* **3**, 25 (1989).
- [42] D. Hartich, A. C. Barato, and U. Seifert, *New Journal of Physics* **17**, 055026 (2015).
- [43] R. Chen, S. Neri, and L. J. Prins, *Nature Nanotechnology* **15**, 868 (2020).
- [44] G. Ragazzon and L. J. Prins, *Nature nanotechnology* **13**, 882 (2018).
- [45] M. M. Lin, *Physical Review Letters* **125**, 218101 (2020).
- [46] S. Liang and S. Pigolotti, *Physical Review E* **108**, L062101 (2023).
- [47] F. Schlögl, *Zeitschrift für Physik* **253**, 147 (1972).
- [48] B. Qureshi, J. M. Poulton, and T. E. Ouldridge, “Information propagation in far-from-equilibrium molecular templating networks is optimised by pseudo-equilibrium systems with negligible dissipation,” (2024), arXiv:2404.02791 [cond-mat, physics:physics, q-bio].
- [49] P. Sartori and S. Pigolotti, *Physical Review X* **5**, 041039 (2015).
- [50] A. Chakrabarti, L. Miskovic, K. C. Soh, and V. Hatziz

- manikatis, *Biotechnology Journal* **8**, 1043 (2013).
- [51] A. Genthon, C. D. Modes, F. Jülicher, and S. W. Grill, “Non Equilibrium Transitions in a Polymer Replication Ensemble,” (2024), arXiv:2403.05665 [cond-mat, physics:physics].
- [52] R. Ravasio, K. Husain, C. G. Evans, R. Phillips, M. Ribezzi, J. W. Szostak, and A. Murugan, “A minimal scenario for the origin of non-equilibrium order,” (2024), arXiv:2405.10911 [cond-mat, q-bio].
- [53] J. H. Rosenberger, T. Göppel, P. W. Kudella, D. Braun, U. Gerland, and B. Altaner, *Physical Review X* **11**, 031055 (2021).
- [54] A. V. Tkachenko and S. Maslov, *The Journal of Chemical Physics* **143**, 045102 (2015).
- [55] S. Toyabe and D. Braun, *Physical Review X* **9**, 011056 (2019).